Determination of the Thresholds in the Split-Step Wavelet Method to Assess Accuracy for Long-Range Propagation

Thomas Bonnafont, Rémi Douvenot, and Alexandre Chabory

Abstract – The split-step wavelet method is a method for computing the tropospheric long-range propagation of electromagnetic waves. It follows the same steps as the split-step Fourier method, but the propagation is performed in the wavelet domain instead of the Fourier domain. The efficiency of this method is based on the fast wavelet transform of low complexity and on sparse representation using compression. Nevertheless, the compression introduces an error that accumulates with iteration. In this article, we propose a closed-form formula for the error that allows a priori computation of the compression thresholds for a given scenario and accuracy. Numerical experiments show the relevance of the proposed approach.

1. Introduction

Tropospheric long-range propagation is a topic of major interest for numerous applications in communication, surveillance, and navigation. The parabolic wave equation model [1] is widely used in this context. In the literature, the parabolic wave equation is iteratively solved with the split-step Fourier method (SSF) by going back and forth in the spectral and spatial domains [2, 3]. This method allows large steps to be made in the propagation direction [1].

To accelerate the computation, wavelet-based methods have been proposed in optics [4] and electromagnetics [5–7]. Recently, an efficient split-step wavelet method (SSW) [6–8] was introduced to solve the parabolic wave equation in electromagnetics in both 2D and 3D. This method computes the field by marching on in distances as SSF, but the propagation is performed in the wavelet domain instead of the spectral domain. Each iteration follows two steps. First, the field is decomposed in the wavelet domain and compressed, introducing the signal compression error (threshold V_{s}). Second, the coefficients are propagated using a compressed wavelet-to-wavelet propagator, introducing the propagator compression error (threshold V_{p}). These errors accumulate throughout the propagation and need to be quantified. Indeed, Zhou et al. [6] have shown that SSW is faster than SSF if good compression is performed.

The main contribution of this article is that we derive a theoretical formula of the accumulated compression error after N_x iterations. This allows us to set both thresholds a priori for a given accuracy and scenario. We also show that the heuristic formula proposed in earlier works [6, 9] is too optimistic.

For conciseness, the method and the proof are developed in 2D. Nevertheless, the results remain valid in 3D using similar calculations. After a general presentation of SSW (Section 2), the error formula is derived (Section 3) and tested via numerical experiments (Section 4) in 2D.

Manuscript received 10 November 2021.

Thomas Bonnafont was with ENAC, Université de Toulouse, France, and is now with ENSTA Bretagne, 2 rue François Verny, 29200 Brest, France; e-mail: thomas.bonnafont@ensta-bretagne.fr.

Rémi Douvenot and Alexandre Chabory are with ENAC, Université de Toulouse, France, 7 avenue Edouard Belin, Toulouse, France; e-mail: remi.douvenot@enac.fr, alexandre.chabory@enac.fr.

2. Overview of the Split-Step Wavelet Method

2.1 Configuration and Discretization

In this article, an $\exp(j\omega t)$ time dependence is assumed, where ω is the angular frequency. The domain is 2D, of size $[0, x_{\max}]$ in x and $[0, z_{\max}]$ in z. The field is known at $x = 0$ and the source is placed at $x \leq 0$. On the z-axis a sampling is made with $z_{p_z} = p_z \Delta z$ and $p_z \in \{0, \ldots, N_z - 1\}$. On the x-axis a sampling is made with $x_{p_x} = p_x \Delta x$ and $p_x \in \{0, \ldots, N_x - 1\}$.

2.2 Brief Reminder of the Discrete Wavelet Transform

The wavelet family is computed by dilating and translating a mother wavelet of zero mean on L levels [10]. Dilations allow covering of the lower parts of the spectrum. To obtain an orthonormal basis, a scaling function of nonzero mean is added. This function covers the lowest part of the spectrum. Using this basis, a multilevel decomposition is obtained. We recall one important property of the wavelets used in the following demonstrations. The number of vanishing moments n_{v} of a wavelet ψ is defined as

$$\forall k \in [0, n_{\mathrm{v}}], \qquad \int z^k \psi(z) dz = 0 \tag{1}$$

This property describes how well a wavelet decomposition can approach a smooth function with few coefficients.

2.3 An Overview of SSW

SSW computes the field iteratively by going back and forth from the wavelet domain to the spatial domain. As with SSF, the refraction and relief are taken into account in the spatial domain, and thus we describe only the free-space propagation part. The initial field u_0 is supposed known.

Denoting by u_{p_x} the field and by U_{p_x} its wavelet decomposition at distance $p_x\Delta x$, a step of SSW is computed as follows. First the wavelet coefficients U_{p_x} are computed by applying a fast wavelet transform on u_{p_x} (denoted $\mathbf{W}$). Then the coefficients are compressed (operator C_{V_s}) with a hard threshold V_s (i.e., all coefficients below V_s are set to 0). A sparse vector of size N_z is obtained. This first compression repeated on N_x horizontal steps induces an error term denoted by $\delta^{\mathrm{s}}_{N_x}$.

Then the coefficients are propagated using a precomputed matrix $\mathbf{P}$:

$$U_{p_x+1} = \mathbf{P} C_{V_s} U_{p_x} \tag{2}$$

This sparse matrix contains all the wavelet-to-wavelet propagations and is of size (N_z, N_z) [6]. A compression with hard threshold V_{p} is performed. Iterated N_x times, this second error term in the method is denoted by $\delta^{\mathrm{m}}_{N_x}$. The free-space propagated field is obtained by coming back in the space domain using an inverse fast wavelet transform. The total compression error is denoted by $\delta_{N_x} = \delta^{\mathrm{s}}_{N_x} + \delta^{\mathrm{m}}_{N_x}$.

In [6] the experimental upper bound was supposed to follow $N_x^{0.5} V_s$ and $N_x V_{\mathrm{p}}$ for the signal and propagator compressions, respectively. We derive here new and more accurate expressions.

3. Derivation of the Compression-Error Formula

In the following section, we introduce the normalized thresholds v_s and v_{p} such that $V_s = v_s \|U_0\|_\infty$ and $V_{\mathrm{p}} = v_{\mathrm{p}} \|\mathbf{P}\|_{\max}$ [10, 11]. We also note that the operator norm of $\mathbf{P}$ corresponds to

$$\|\mathbf{P}\|_{\mathrm{op}} = \sup_{U \neq 0} \|\mathbf{P}U\|_2 \big/ \|U\|_2 \tag{3}$$

From power conservation, the operator norm of the free-space propagator $\mathbf{P}$ is equal to 1 $\left(\|\mathbf{P}\|_{\mathrm{op}} = 1\right)$. If there are no evanescent waves and the propagation does not reach any boundaries, then we have $\|\mathbf{P}u\|_2 = \|u\|_2$. In other cases (apodization, environment losses, evanescent waves, and so on), then we have $\|\mathbf{P}u\|_2 \leq \|u\|_2$.

3.1 Signal Compression Error

The objective of this section is to study how the signal compression error accumulates with N_x. We first assume that $V_s \neq 0$ and $V_{\mathrm{p}} = 0$. The propagator has no compression. The error due to the threshold V_s on the signal (operator C_{V_s}) after N_x iterations is defined by

$$\delta^{\mathrm{s}}_{N_x} = \left\| \tilde{U}_{N_x} - U_{N_x} \right\|_2 \Big/ \|U_0\|_2 \tag{4}$$

with $\tilde{U}_{N_x} = (\mathbf{P} C_{V_s})^{N_x} U_0$ and $U_{N_x} = \mathbf{P}^{N_x} U_0$ the compressed and uncompressed propagated coefficients, respectively.

For one iteration, the error is given by

$$\delta^{\mathrm{s}}_1 = \|\mathbf{P} C_{V_s} U_0 - \mathbf{P} U_0\|_2 \big/ (U_0]_2 \tag{5}$$

We introduce ε_0, the compression term due to C_{V_s} defined by

$$C_{V_s} U_0 = U_0 + \epsilon_0 \tag{6}$$

Using (3) and introducing (6) into (5), we obtain $\delta^{\mathrm{s}}_1 \leq \|\epsilon_0\|_2 / \|U_0\|_2$. For the smooth signals we are manipulating, the wavelet coefficients decrease exponentially to 0 [10, 11]. Therefore, we rewrite the norm of the error as

$$\|\epsilon\|_2^2 = v_s^2 \|U_0\|_\infty^2 \sum_{m=0}^{N_z - M - 1} \left|\hat{\epsilon}^0_m\right|^2 \tag{7}$$

with the coefficients $\left|\hat{\epsilon}^0_m\right| \leq 1$ corresponding to the normalized amplitudes of the wavelet coefficients of the error indexed in decreasing order, and $M \ll N_z$ the number of significant coefficients. Following [10–12], error components are bounded by

$$\left|\hat{\epsilon}^0_m\right| \leq C_\epsilon (m+1)^{-n_{\mathrm{v}}} \tag{8}$$

with $m \in [0, N_z - M - 1]$, n_{v} the number of vanishing moments, and C_ϵ a constant depending only on the smoothness of the field and of the wavelets. Putting (8) in (7), an upper bound for $\|\epsilon_0\|_2$ is obtained:

$$\|\epsilon_0\|_2 \leq v_s \|U_0\|_\infty C_\epsilon \sqrt{\sum_{m=0}^{N_z - M - 1} (m+1)^{-2n_{\mathrm{v}}}} \tag{9}$$

For $n_{\mathrm{v}} \geq 2$, the sum converges close to 1 (e.g., for $n_{\mathrm{v}} = 2$ it is about 1.082). Also, C_ϵ is less than or close to 1, as illustrated with numerous numerical tests in Section 4 and in [13].

Thus, the bound on the error due to signal compression after one iteration is given by

$$\|\epsilon_0\|_2 \lesssim v_s \|U_0\|_2 \quad \text{and} \quad \delta^{\mathrm{s}}_1 \lesssim v_s \tag{10}$$

where $\lesssim$ means less than or close to, as widely used in the wavelet community [10, 11]. In practice, this result shows very good accuracy, with numerous numerical tests performed in [6, 14].

For two iterations, we compare the propagations with and without compression:

$$\delta^{\mathrm{s}}_2 = \|(\mathbf{P} C_{V_s})(\mathbf{P} C_{V_s}) U_0 - \mathbf{P}\mathbf{P} U_0\|_2 \big/ \|U_0\|_2 \tag{11}$$

We define the second compression error ϵ_1 as $C_{V_s}(\mathbf{P}U_0 + \mathbf{P}\epsilon_0) = \mathbf{P}U_0 + \mathbf{P}\epsilon_0 + \epsilon_1$. The expression of the error is calculated as

$$\delta_2^{\mathrm{s}} = \|\mathbf{PP}U_0 + \mathbf{PP}\epsilon_0 + \mathbf{P}\epsilon_1 - \mathbf{PP}U_0\|_2 \big/ \|U_0\|_2$$
$$\leq \big(\|\epsilon_0\|_2 + \|\epsilon_1\|_2\big) \big/ \|U_0\|_2 \tag{12}$$

Supposing (10) is true for the second iteration, we obtain

$$\|\epsilon_1\|_2 \big/ \|U_0\|_2 \lesssim v_{\mathrm{s}} \big(\|U_0\|_2 + \|\epsilon_0\|_2\big) \big/ \|U_0\|_2 \tag{13}$$

Since, with an appropriate threshold, $\|\epsilon_0\|_2$ is negligible to $\|U_0\|_2$, we have $\delta_2^{\mathrm{s}} \lesssim 2v_{\mathrm{s}}$. By induction, the signal compression error after N_x horizontal iterations fulfills

$$\delta_{N_x}^{\mathrm{s}} \lesssim N_x v_{\mathrm{s}} \tag{14}$$

The appropriate threshold $V_{\mathrm{s}} = v_{\mathrm{s}} \|U_0\|_\infty$ can now be computed with (14). The same study is now performed on the error due to the compression of the propagator $\mathbf{P}$ in (2).

3.2 Propagator Compression Error

We now assume that $V_{\mathrm{s}} = 0$ and $V_{\mathrm{p}} \neq 0$. The error $\delta_{N_x}^{\mathrm{p}}$ due to the compression of the propagator after N_x iterations is studied. It is defined by

$$\delta_{N_x}^{\mathrm{p}} = \left\| \tilde{U}_{N_x} - U_{N_x} \right\|_2 \Big/ \|U_0\|_2 \tag{15}$$

where $\tilde{U}_{N_x}$ corresponds to the coefficients propagated N_x times with the compressed operator denoted as $\mathbf{P} + \Delta\mathbf{P}$.

From [11, pp. 29–32], we have the norm operator of $\Delta\mathbf{P}$ bounded by

$$\|\Delta\mathbf{P}\|_{\mathrm{op}} = \sup_{U \neq 0} \|\Delta\mathbf{P}U\|_2 \big/ \|U\|_2 \leq v_{\mathrm{p}} \tag{16}$$

For one iteration, the expression of the error is given by

$$\delta_1^{\mathrm{p}} = \left\| \tilde{U}_1 - U_1 \right\|_2 \Big/ \|U_0\|_2 = \|\Delta\mathbf{P}U_0\|_2 \big/ \|U_0\|_2 \tag{17}$$

Following (16), we have $\delta_1^{\mathrm{p}} \leq v_{\mathrm{p}}$ in agreement with Kremp and Freude [4].

Using the same notations and methodology as for one iteration, and since $\|\mathbf{P}\|_{\mathrm{op}} = 1$, using (16) we obtain for two iterations

$$\begin{aligned}\delta_2^{\mathrm{p}} &= \left\| \tilde{U}_2 - U_2 \right\|_2 \Big/ \|U_0\|_2 \\ &\leq \frac{\|\Delta\mathbf{PP}U_0\|_2 + \|\mathbf{P}\Delta\mathbf{P}U_0\|_2 + \left\|\Delta\mathbf{P}^2 U_0\right\|_2}{\|U_0\|_2} \leq 2v_{\mathrm{p}} + v_{\mathrm{p}}^2\end{aligned} \tag{18}$$

Neglecting the term v_{p}^2 $\left(v_{\mathrm{p}} \ll 1\right)$, we see that δ_2^{m} is less than or close to $2v_{\mathrm{p}}$. By induction, we finally obtain

$$\delta_{N_x}^{\mathrm{p}} \lesssim v_{\mathrm{p}} N_x \tag{19}$$

From (19), we are able to choose the adequate threshold V_{p} for a given error and scenario.

Assuming that both errors are independent, we finally derive a closed-form expression for the accumulated compression error $\delta_{N_x} \lesssim \left(v_{\mathrm{s}} + v_{\mathrm{p}}\right) N_x$. In practice, for a given maximum expected error $\delta_{N_x}^{\max}$ and number of iterations N_x, the normalized thresholds are computed as

$$v_{\mathrm{s}} = \delta_{N_x}^{\max} \Big/ (2N_x) \quad \text{and} \quad v_{\mathrm{p}} = \delta_{N_x}^{\max} \Big/ (2N_x) \tag{20}$$

Thus we derive the unnormalized thresholds

$$V_{\mathrm{s}} = \frac{\delta_{N_x}^{\max}}{2N_x} \|U_0\|_\infty \quad \text{and} \quad V_{\mathrm{p}} = \frac{\delta_{N_x}^{\max}}{2N_x} \|\mathbf{P}\|_{\max} \tag{21}$$

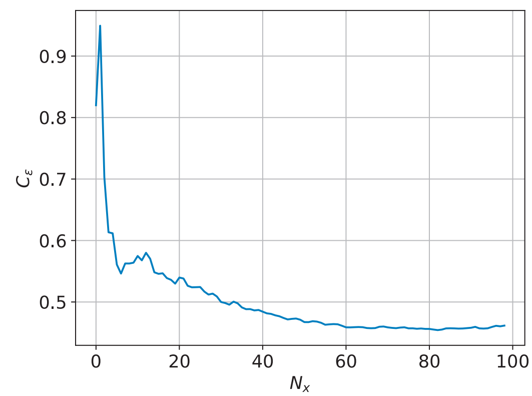

Figure 1. Evolution of C_ϵ with N_x.

4. Numerical Tests

In this section, numerical experiments are performed to show that the thresholds v_{s} and v_{p} can be managed to assess a given final accuracy for a certain number of iterations N_x, using (20). First, a short-range simulation in free space is performed to assess the accuracy of the formulas. Second, we perform a long-range simulation with relief and refraction.

4.1 Free-Space Scenario

We perform the tests in 2D. The source is a uniform aperture at $f_0 = 300$ MHz of size 10 m placed at $z_{\mathrm{s}} = 1024$ m in a domain of vertical size $z_{\max} = 2048$ m. The domain is of horizontal size $x_{\max} = 2000$ m. The step sizes are $\Delta x = 20$ m and $\Delta z = 0.5$ m. Thus, we have $N_x = 100$. For the wavelet parameters, the symlet with $n_v = 6$ and a maximum level of $L = 3$ is chosen.

The root-mean-square error between compressed and uncompressed propagations is computed for different values of N_x and compared to the closed-form formulas. Thresholds are set to $v_{\mathrm{s}} = v_{\mathrm{p}} = 1.6 \times 10^{-4}$ using (20), so as to obtain an error of –30 dB at the final range.

First, as shown in Figure 1, we compute and plot the constant $C_\epsilon \simeq \|\epsilon\|_2 \big/ V_{\mathrm{s}}$ at each step N_x. This shows that the constant is less than or close to 1, which corroborates the approximation leading to (14) proposed in Section 3.1.

The root-mean-square error is computed and given in Figure 2. As expected, the closed-form formula for the compression error is never reached. The

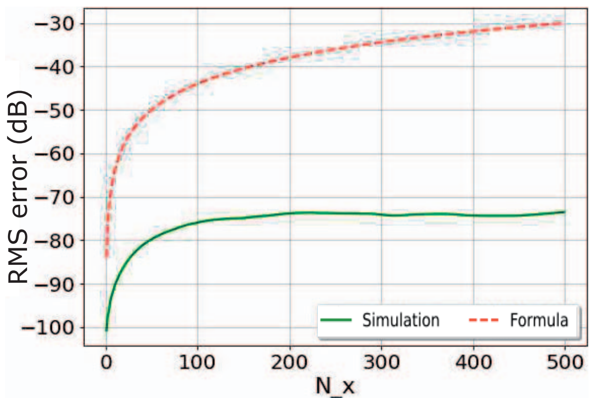

Figure 2. Evolution of the root-mean-square error.

computed thresholds allow the error to be bounded below the desired maximum. We also compute a linear regression to find the optimal α such that $\delta^{\mathrm{s}}_{N_x} \sim v_{\mathrm{s}} N_x^{\alpha}$ and $\delta^{\mathrm{p}}_{N_x} \sim v_{\mathrm{p}} N_x^{\alpha}$. For the signal compression, we obtain $\alpha = 0.96$, slightly lower than the value proposed here—i.e., 1—but greater than the heuristic value (0.5) proposed in [6]. This shows that the heuristic formula proposed in [6] was too optimistic. For the propagator, we obtain $\alpha = 0.97$, close to the value proposed here and in [6].

This illustrates the relevance of the proposed formulas (20). Therefore, they can be used to tune the thresholds needed in SSW to obtain a given accuracy. In the next section, a numerical test in realistic conditions is performed.

4.2 Realistic Scenario

The propagation of a complex source point in a domain with a trilinear atmosphere and two triangular reliefs is computed. The parameters of the complex source point are frequency $f = 300$ MHz, coordinates $x_{w0} = -50$ m and $z_{\mathrm{s}} = 50$ m, and waist size $W_0 = 5$ m. We consider an atmosphere described by a trilinear duct [15] of base height $z_{\mathrm{b}} = 241$ m, thickness $z_{\mathrm{t}} = 391$ m, and gradient $c_2 = -0.5$ M-units/m in the duct and $c_0 = 0.118$ M-units/m elsewhere. On the ground, we choose $M_0 = 330$ M-units. The relief is chosen as two small triangles of heights 100 m and 200 m. The impedance ground has parameters $\varepsilon_r = 20.0$ and $\sigma = 0.02$ S/m.

The domain is of horizontal size $x_{\max} = 100$ km and vertical size $z_{\max} = 2048$ m. An apodization window is added on top of the domain. The grid size is 200 m horizontal and 0.5 m vertical. We aim at obtaining an error of –30 dB at the final iteration. From (20) we apply the thresholds $v_{\mathrm{s}} = v_{\mathrm{p}} = 3.16 \times 10^{-5}$.

In Figure 3, the field (in decibel-volts per meter) is plotted in (a) and the root-mean-square error evolution is plotted in (b). We can see that the bound is not reached and that the final error is significantly smaller than the desired error. This is mostly due to the apodization layer, in which energy is leaving the

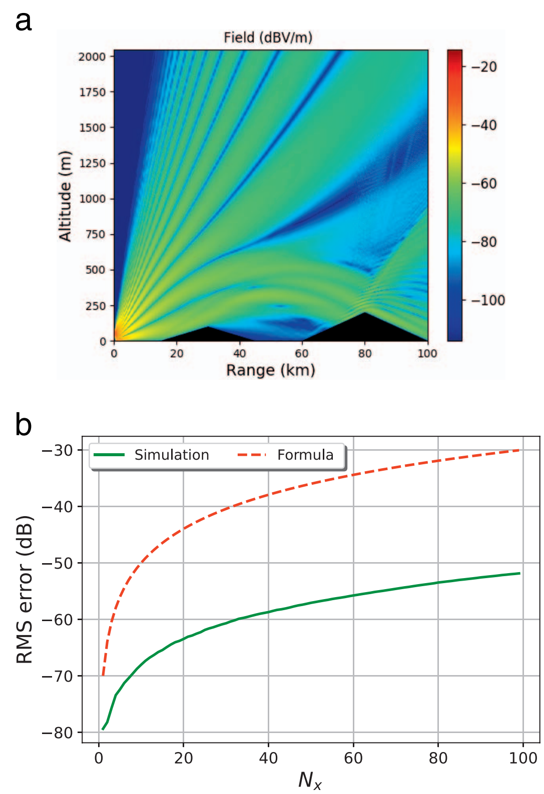

Figure 3. Results for the realistic test case. (a) Field obtained with the split-step wavelet method (in decibel-volts per meter); (b) root-mean-square error (in decibels).

computational domain, reducing the total error. Therefore, our formula is conservative in a realistic domain.

5. Conclusion

In this article, we have derived a closed-form expression for the accumulated compression error in the split-step wavelet method (SSW). This formula allows the thresholds V_{s} and V_{p} to be tuned for a given accuracy.

First, we gave an overview of SSW to show where thresholds are applied. The compressions V_{s} on the signal and V_{p} on the propagator introduce errors. We derived how each error accumulates during iteration to obtain a conservative expression for the compression error. This latter allows us to set V_{s} and V_{p} a priori for a given accuracy and scenario. Finally, numerical tests in 2D were performed.

To conclude, the expression obtained in this article for the accumulated compression error is now successfully used in SSW [8] to tune V_{s} and V_{p} for a given scenario.

6. References

1. M. Levy, *Parabolic Equation Methods for Electromagnetic Wave Propagation*, London, IET, 2000.
2. D. Dockery and J. R. Kuttler, "An Improved Impedance-Boundary Algorithm for Fourier Split-Step Solutions of

the Parabolic Wave Equation," *IEEE Transactions on Antennas and Propagation*, **44**, 12, December 1996, pp. 1592-1599.

3. J. R. Kuttler and R. Janaswamy, "Improved Fourier Transform Methods for Solving the Parabolic Wave Equation," *Radio Science*, **37**, 2, April 2002, pp. 1-11.
4. T. Kremp and W. Freude, "Fast Split-Step Wavelet Collocation Method for WDM System Parameter Optimization," *Journal of Lightwave Technology*, **23**, 3, 2005, pp. 1491-1502.
5. A. Iqbal and V. Jeoti, "An Improved Split-Step Wavelet Transform Method for Anomalous Radio Wave Propagation Modeling," *Radioengineering*, **23**, 4, December 2014, pp. 987-996.
6. H. Zhou, R. Douvenot, and A. Chabory, "Modeling the Long-Range Wave Propagation by a Split-Step Wavelet Method," *Journal of Computational Physics*, **402**, February 2020, p. 109042.
7. T. Bonnafont, R. Douvenot, and A. Chabory, "A Local Split-Step Wavelet Method for the Long Range Propagation Simulation in 2D," *Radio Science*, **56**, 2, 2021, p. e2020RS007114.
8. T. Bonnafont, R. Douvenot, and A. Chabory, "Split-Step Wavelet with Local Operators for the 3D Long-Range Propagation," 2021 15th European Conference on Antennas and Propagation (EuCAP), Dusseldorf, Germany, March 22–26, 2021, pp. 1-5.
9. H. Zhou, *Modeling the Atmospheric Propagation of Electromagnetic Waves in 2-D and 3-D Using Fourier and Wavelet Transforms*, Ph.D. dissertation, Université Paul Sabatier - Toulouse III, France, 2018.
10. S. Mallat, *A Wavelet Tour of Signal Processing*, 2nd Ed., San Diego, CA, Academic Press, 1999.
11. A. Cohen, *Numerical Analysis of Wavelet Methods*, Amsterdam, the Netherlands, Elsevier, 2003.
12. R. A. DeVore, B. Jawerth, and V. Popov, "Compression of Wavelet Decompositions," *American Journal of Mathematics*, **114**, 4, August 1992, pp. 737-785.
13. T. Bonnafont, *Modeling the Atmospheric Long-Range Electromagnetic Waves Propagation in 3D Using the Wavelet Transform*, Ph.D. dissertation, Université Paul Sabatier - Toulouse III, France, 2020.
14. T. K. Sarkar, M. Salazar-Palma, and M. C. Wicks, *Wavelet Applications in Engineering Electromagnetics*, Boston, MA, Artech House, 2002.
15. E. E. Gossard and R. G. Strauch, "*Radar observation of clear air and clouds,*" Elsevier, New York, 1983.